Unbinding Transition of Probes in Single-File Systems

Olivier Bénichou,[1] Vincent Démery,[2,3] and Alexis Poncet[1,4]
[1]Laboratoire de Physique Théorique de la Matière Condensée, CNRS/UPMC, 4 Place Jussieu, F-75005 Paris, France
[2]Gulliver, CNRS, ESPCI Paris, PSL Research University, 10 rue Vauquelin, 75005 Paris, France
[3]Univ Lyon, ENS de Lyon, Univ Claude Bernard Lyon 1, CNRS, Laboratoire de Physique, F-69342 Lyon, France
[4]Département de Physique, ENS, PSL Research University, 24 Rue Lhomond, 75005 Paris, France

(Received 19 July 2017; revised manuscript received 17 October 2017; published 16 February 2018)

Single-file transport, arising in quasi-one-dimensional geometries where particles cannot pass each other, is characterized by the anomalous dynamics of a probe, notably its response to an external force. In these systems, the motion of several probes submitted to different external forces, although relevant to mixtures of charged and neutral or active and passive objects, remains unexplored. Here, we determine how several probes respond to external forces. We rely on a hydrodynamic description of the symmetric exclusion process to obtain exact analytical results at long times. We show that the probes can either move as a whole, or separate into two groups moving away from each other. In between the two regimes, they separate with a different dynamical exponent, as $t^{1/4}$. This unbinding transition also occurs in several continuous single-file systems and is expected to be observable.

DOI: 10.1103/PhysRevLett.120.070601

Single-file transport arises in systems as varied as ionic channels [1], nanotubes [2–6], and zeolites [7]. The hallmark of these systems does not lie in the collective dynamics, which is simply diffusive, but in the motion of individual probes [8,9]. In the absence of an external force, a single probe diffuses anomalously due to the interactions with its neighbors, its mean squared displacement scaling as $\langle X(t)^2\rangle \sim \sqrt{t}$ [7,9–13]. In response to a constant external force, its displacement evolves as $X(t) \sim \sqrt{t}$, in agreement with the fluctuation-dissipation theorem [14,15]. The probability density function of the probe is Gaussian at long times. Finite time corrections have recently been determined [16], and generalized to systems with an initial density gradient [17] or to a driven probe [18,19]. Remarkably, a driven probe drags with it the surrounding particles, which can be seen as "bound" to the probe [18].

In contrast, the effects involving several driven probes remain unexplored, despite their relevance to the situations described above. An especially important example concerns the ionic transport through subnanometer carbon nanotubes [6]. Indeed, in these nanotubes, water molecules are confined to a single-file chain [2,6], and ions act as driven particles if a potential difference is applied between the reservoirs.

Here, we determine the response of several probes to external forces [Figs. 1(a),2(a),3(a)]. We show that the bonds induced by the single-file geometry can be broken; we characterize this unbinding transition, and explain its impact on the motion of the probes. We obtain exact results for the average positions of the probes in the simple exclusion process (SEP), which is a paradigmatic model of single-file systems. These conclusions are shown to also apply to model colloidal systems used in experiments [9,13], which points towards their universality.

In the SEP, particles move on a one-dimensional lattice with step a; single-file diffusion is enforced by allowing at most one particle per site [Fig. 1(b)]. The density ρ is the proportion of occupied sites. Each particle can jump to the left or to the right, with rates $1/(2\tau)$. For the probes, these rates are modified: a probe submitted to an external force f jumps to the left and to the right with rates $(1-s)/(2\tau)$ and $(1+s)/(2\tau)$, respectively, where $s = \tanh(af/[2k_BT])$ is set by detailed balance. Note that the gas of pointlike Brownian particles at density $\hat{\rho}$ is recovered as the limit of the SEP at vanishing density, $\rho \to 0$, with $\hat{\rho} = \rho/a$ kept constant.

First, we focus on the asymmetric case with two probes [Fig. 1(a)]. Initially located at $X_1(0) = -L/2$ and $X_2(0) = L/2$, with $L \gg a$, with a uniform density ρ_∞ of unbiased particles, they are submitted to forces $f_1 = -f_2 = -f$. We performed numerical simulations [20] and observed two behaviors: they can either remain bound, or unbind and move away from each other, their displacement being proportional to $\sqrt{t}$ [Figs. 1(c), 1(d)]. In the bound state, the equilibrium distance between the probes increases with the force and diverges upon approaching a critical force; conversely, the factor of $\sqrt{t}$ in the unbound state decays to zero as the critical force is approached from above [Fig. 1(e)]. At the critical force, the probes separate with a different exponent [Fig. 1(d)].

Two probes submitted to external forces f_1 and f_2 can also be bound, and move together as $\sqrt{t}$, or unbound, and move as $A_i\sqrt{t}$ with $A_1 \neq A_2$ [Figs. 2(a), 2(c)]. Their state can be represented in a phase diagram [Fig. 2(b)]. Upon approaching the unbinding transition from above and

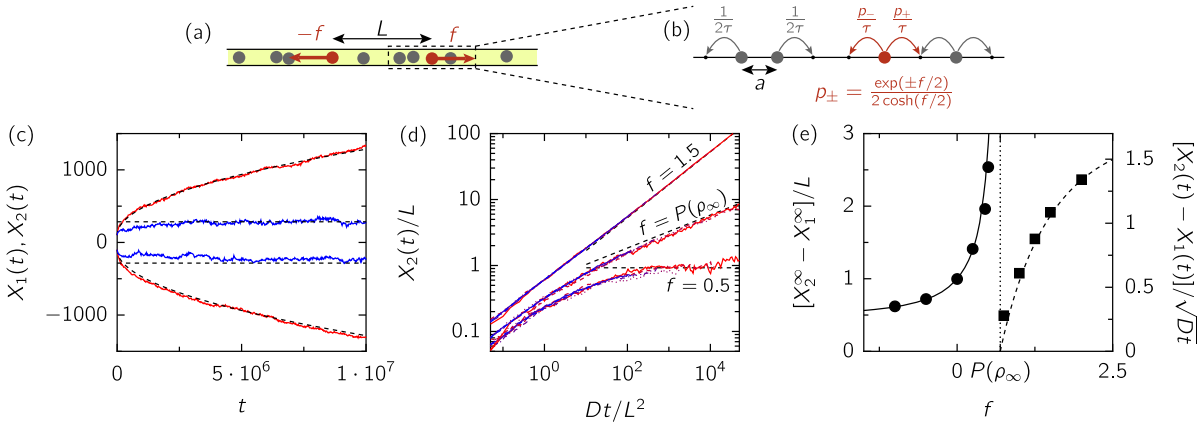

FIG. 1. Two probes submitted to opposite forces in a single file system. (a) General scheme: two probes (red) in a single file system (bath particles in grey) initially at a distance L are submitted to opposite forces $\mp f$. (b) Possible moves and transition rates in the SEP with biased probes (red). (c) Example of trajectories for $f = 0.5$ (blue) and $f = 1.5$ (red), for $\rho_\infty = 0.5$. The dashed black lines are the theoretical predictions. Distances are given in units of a and forces in units of k_BT/a. (d) Rescaled trajectory of the probe 2 in log-log scale for $f = 0.5$, $P(\rho_\infty) \simeq 0.69$, 1.5, and $L = 10$, 20, 50, 100, 200, 500 (red to blue). (e) Separation of the probes in the bound $[f < P(\rho_\infty)$, filled circle] and unbound $[f > P(\rho_\infty)$, filled square] regimes. Points are the results of numerical simulations and the lines are the theoretical results (6) and (7).

below, the same behavior as in the antisymmetric case is found [Fig. 2(d)]. Interestingly, in the bound state the "velocity" of the probes depends only on the sum of the forces, $f_1 + f_2$; when they unbind, the velocity of the center of mass decreases rapidly [Fig. 2(e)]. Finally, N driven probes can also be bound and move as a whole [Fig. 3(c)] or separate into two groups [Fig. 3(e)].

We have run numerical simulations of other systems, focusing on the model systems used in experiments. Systems implementing the single-file property have been realized with colloids confined to a narrow channel either printed in the substrate [9,13], or generated with scanning optical tweezers [12]. The colloids either interact through a magnetic dipolar interaction, as $1/r^3$, where r is the

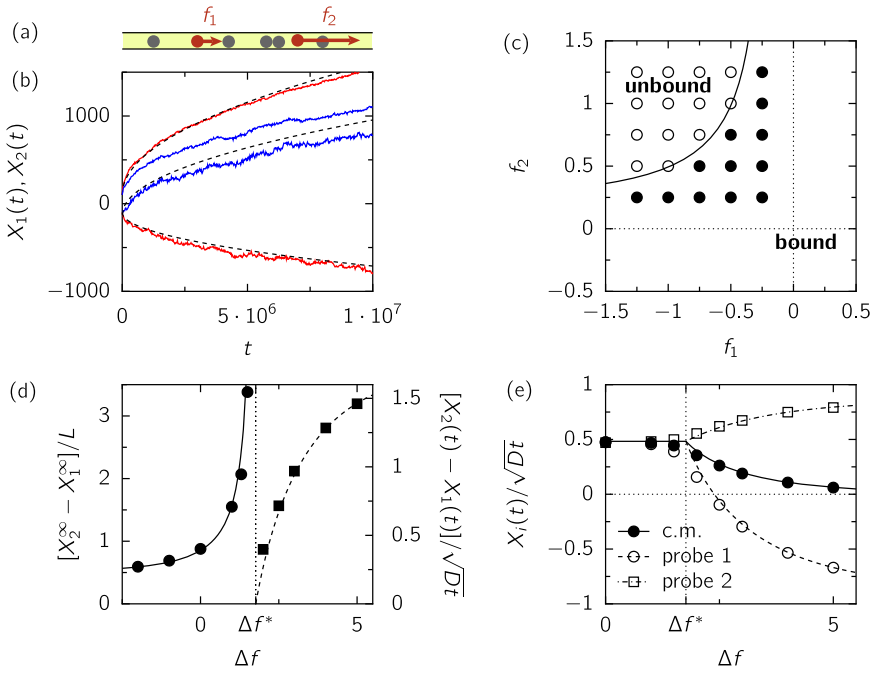

FIG. 2. Two probes submitted to arbitrary forces. (a) Two probes located at $X_1 < X_2$ are submitted to arbitrary forces f_1 and f_2. (b) Two examples of trajectories for $f_1 = 0$, $f_2 = 1$ (blue) and $f_1 = -1$, $f_2 = 2$ (red). (c) Phase diagram: bound (filled circle) and unbound (circle) configurations, the line is the theoretical prediction (12), (13). (d) Separation in the bound (filled circle) and unbound (filled square) regimes for $F = f_1 + f_2 = 1$ as a function of the force difference $\Delta f = f_2 - f_1$; Δf^* is the critical force difference [Eqs. (12), (13)]. (e) Motion of each probe, and of the center of mass (c.m.) for the same parameters.

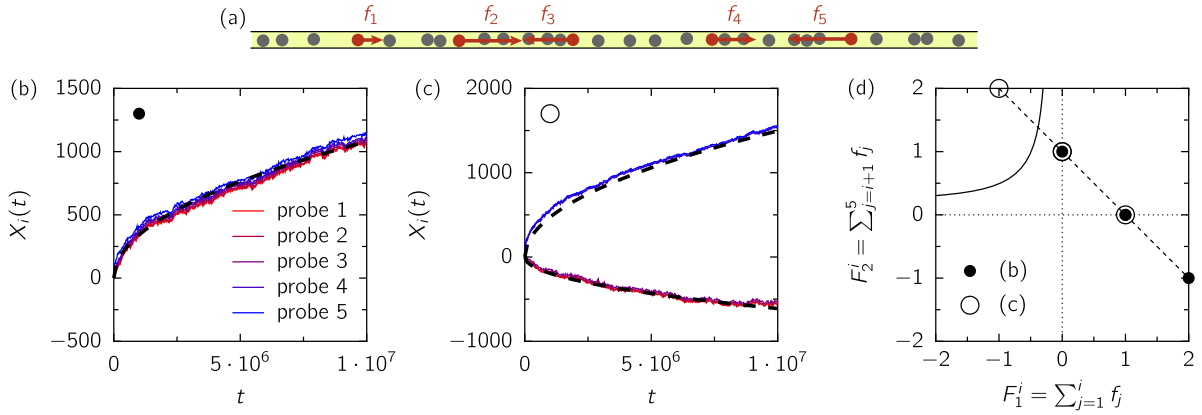

FIG. 3. Five probes submitted to arbitrary forces (a). (b),(c) Simulated trajectories and theoretical predictions (black dashed lines) for forces $(1, 1, -1, -1, 1)$ (b) and $(1, -1, -1, 1, 1)$ (c). (d) Two probes phase diagram for $\rho = 0.5$; it shows that all the possible divisions remain bound in case b (filled circle) and that the groups (1,2,3) and (4,5) unbind in case c (circle).

interparticle distance [9], or behave as hard rods, as in the Tonks' gas [13]. We simulated these two systems with an overdamped dynamics, inserting two probes submitted to opposite forces, and found the same phenomenology as in the SEP (Fig. 4).

To account for these observations, we start from the hydrodynamic description of the SEP introduced in Refs. [14,15] to investigate the response of a single probe to a constant force. Notably, this approach gives the exact result for the mean position of the probe and the density profile of the bath particles at long time. The starting point of the analysis is that the bath density $\rho(x, t)$ has a diffusive behavior [22],

$$\frac{\partial \rho}{\partial t}(x, t) = D \frac{\partial^2 \rho}{\partial x^2}(x, t), \tag{1}$$

where the diffusion coefficient is $D = a^2/(2\tau)$. The probe i, located at $X_i(t)$ in average, acts as a moving wall

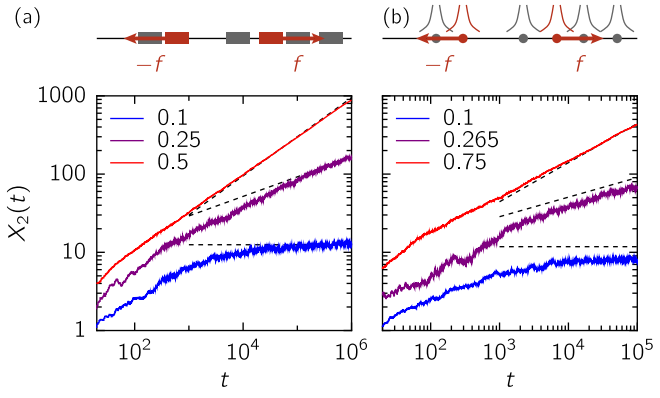

FIG. 4. Two probes submitted to opposite forces in the Tonks' gas (a) and the dipolar gas (b). Trajectory of the probe 2 in the Tonks' gas of hard rods (a) and in the dipolar gas with $1/r^3$ interactions (b) at $\rho_\infty = 0.2$, for different values of the force f (solid lines). In the Tonks' gas, $P(\rho_\infty) = 0.25$; in the dipolar gas, $P(\rho_\infty) \simeq 0.265$. The dashed black lines are the theoretical predictions [20].

that imposes a no-flux boundary condition, namely, $D(\partial\rho/\partial x)(X_i^\pm, t) = -\rho(X_i^\pm, t)(dX_i/dt)$.

The several probes situation is conveniently analyzed by first revisiting the single probe case. Within the hydrodynamic approach, it has been shown [14,15] that the densities immediately left and right of a probe moving as

$$X(t) \sim A\sqrt{t} \tag{2}$$

are given by

$$\rho(X^\pm) = \rho_\infty g\left(\pm \frac{A}{2\sqrt{D}}\right), \tag{3}$$

where $g(u) = [1 - \sqrt{\pi} u \exp(u^2)\mathrm{erfc}(u)]^{-1}$. The system of equations is closed with a relation between the velocity of the probe, the force on the probe and the densities on each side of the probe [14,15]. We show in the Supplemental Material [20] that this relation can actually be interpreted as a force balance,

$$f = P[\rho(X^+)] - P[\rho(X^-)], \tag{4}$$

which involves the pressure of the SEP [23],

$$P(\rho) = -\frac{k_B T}{a} \log(1 - \rho). \tag{5}$$

Using Eqs. (3), (4) gives back the implicit equation for A given in Refs. [14,15], which can be solved numerically. As we proceed to show, this new interpretation allows a direct generalization to the case of several driven particles. Moreover, it underlines the robustness of our approach, which can be applied to other single-file systems.

We turn to the situation where two probes are submitted to opposite external forces, $f_2 = -f_1 = f$ (Fig. 1). First, we focus on the case where the probes remain bound, meaning that their positions converge, and we define $X_i^\infty = \lim_{t\to\infty} X_i(t)$ [Figs. 1(c), 1(d)]. In this case, the density between the probes is uniform and we denote it by ρ_1, while

the density outside of the probes is the density at infinity, ρ_∞. The density between the probes is given by Eq. (4), $P(\rho_1) = P(\rho_\infty) - f$, and allows one to compute the equilibrium distance between the probes, $L^\infty = X_2^\infty - X_1^\infty = L\rho_\infty/\rho_1$ [Fig. 1(d)]. This bound state is observed as long as the force f does not exceed the pressure of the outer gas, $P(\rho_\infty)$. As this pressure is approached from below, the distance between the probes diverges as [Fig. 1(e)]

$$\frac{X_2^\infty - X_1^\infty}{L} \underset{f\to P(\rho_\infty)^-}{\sim} \frac{\rho_\infty P'(0)}{P(\rho_\infty) - f} \overset{\text{SEP}}{=} \frac{k_B T \rho_\infty}{a[P(\rho_\infty) - f]}, \quad (6)$$

where $P'(\rho)$ denotes the derivative of the pressure with respect to ρ.

When the forces overcome the pressure of the gas, the probes unbind and move apart as $X_2(t) = -X_1(t) \sim A\sqrt{t}$, and the density between the probes decays to zero. The force balance (4) for the probe 2 together with Eq. (3) give $f = P[\rho_\infty g(A/[2\sqrt{D}])]$, which is an implicit equation for A [Fig. 1(d)]. As f approaches $P(\rho_\infty)$ from above, A decays and [Fig. 1(e)]

$$\frac{X_2(t)}{\sqrt{Dt}} \underset{\substack{t\to\infty \\ f\to P(\rho_\infty)^+}}{\sim} \frac{2}{\sqrt{\pi}} \frac{f - P(\rho_\infty)}{\rho_\infty P'(\rho_\infty)} \quad (7)$$

$$\overset{\text{SEP}}{=} \frac{2}{\sqrt{\pi}} \frac{1-\rho_\infty}{\rho_\infty} \frac{a[f - P(\rho_\infty)]}{k_B T}. \quad (8)$$

Equations (6)–(7) quantify the behavior of the system at the vicinity of the unbinding transition, which occurs at $f = P(\rho_\infty)$. However, they leave aside the important question of what happens at the transition. From Eqs. (6)–(7), we may expect the separation to evolve in time as a power law, $X_2(t) = -X_1(t) \sim Ct^\gamma$, with a different exponent $\gamma \in (0, 1/2)$. Under this assumption, the density $\rho_1(t)$ between the two probes is uniform and $\rho_1(t) \sim L\rho_\infty/(2Ct^\gamma)$. The density in front of the probe 2 can be shown to be given by $\rho(X_2(t)^+, t) - \rho_\infty \propto \rho_\infty C t^{\gamma - \frac{1}{2}}$. Using Eqs. (4), (5) leads to $X_2(t) \propto \sqrt{LP'(0)/P'(\rho_\infty)}\, t^{1/4}$ [20], and the exact expression is

$$X_2(t) \underset{t\to\infty}{\sim} \sqrt{\frac{2\sqrt{\pi}}{B(1/2, 1/4)}} \sqrt{\frac{P'(0)L}{P'(\rho_\infty)}} (Dt)^{1/4} \quad (9)$$

$$\overset{\text{SEP}}{\simeq} 0.82\sqrt{(1-\rho_\infty)L}(Dt)^{1/4}, \quad (10)$$

where B is the beta function [Fig. 1(d)].

It is noteworthy that the dependence of the separation between the probes on the time t and the initial separation L is constrained by the diffusive scaling of the bath in the three regimes. Indeed, the position of the second probe can be written in all regimes as

$$X_2(t) = L\psi(Dt/L^2), \quad (11)$$

with $\psi(u) \sim 1$ if $f < P(\rho_\infty)$, $\psi(u) \sim u^{1/4}$ if $f = P(\rho_\infty)$ and $\psi(u) \sim \sqrt{u}$ if $f > P(\rho_\infty)$ [Fig. 1(d)].

The considerations above can be extended to the case where the two probes are submitted to arbitrary forces f_1 and f_2 [Fig. 2(a)]. When the probes are bound, the density between them becomes uniform and the force balance (4) shows that their displacement is $A\sqrt{t}$, where A is the same as for a single probe submitted to the force $F = f_1 + f_2$ (Figs. 2(c), 2(e), [20]). Unbinding occurs when the forces overcome the pressure of the gas at the left of probe 1 and at the right of probe 2, i.e., when $f_1 = f_1^*(A)$ and $f_2 = f_2^*(A)$ [Fig. 2(c)] with

$$f_1^*(A) = -P\left[\rho_\infty g\left(-\frac{A}{2\sqrt{D}}\right)\right], \quad (12)$$

$$f_2^*(A) = P\left[\rho_\infty g\left(\frac{A}{2\sqrt{D}}\right)\right]. \quad (13)$$

After unbinding, the probes move as $X_i(t) \sim A_i\sqrt{t}$, $A_1 < A_2$, with $f_1 = -P[\rho_\infty g(-A_1/[2\sqrt{D}])]$ and $f_2 = P[\rho_\infty g(A_2/[2\sqrt{D}])]$ [Figs. 2(d), 2(e)]. The displacement of the center of mass does not depend on $\Delta f = f_2 - f_1$ as long as the probes are bound, but it decreases rapidly when they unbind [Fig. 2(e)].

Our results show that two probes that are bound can be seen as a single one, and this statement directly generalizes to N probes [Fig. 3(a)]. Moreover, when the ensemble of N probes separates into two groups moving away from each other, each group can be seen as a single probe. It is actually not possible to have more than two groups, except if there is a group of probes on which the total force is zero: a probe located between two separating probes sees a bath of vanishing density, and thus moves freely in the direction of its force, until it meets the left or right probe. To determine whether the N probes remain bound, the two probes analysis can be applied to the $N-1$ possible divisions of the N probes into two groups. The set of forces to consider are (F_1^i, F_2^i), where $F_1^i = \sum_{j=1}^i f_j$ and $F_2^j = \sum_{j=i+1}^N f_j$, for $1 \le i < N$. If all the points (F_1^i, F_2^i) are in the bound region of the phase diagram in Fig. 2(b), the N probes remain bound [Figs. 3(b), 3(c)]; otherwise, they split for the index i that maximizes $\Delta F^i = F_2^i - F_1^i$ [Figs. 3(d), 3(e)].

Our analytical results are in excellent agreement with numerical simulations. In fact, our results are expected to be exact because (i) the hydrodynamic approach that we used has been shown to give exact results for the mean position of a single probe under a constant force at long times [14,15], and (ii) the motion of several probes that are bound can be computed exactly when the density is close to 1 using an expansion in the number of vacancies similar to the one used in Ref. [24], and confirms our results.

We have provided exact results for the SEP, and have shown that the unbinding transition is robust, as it also takes place in continuous models that represent experimental systems [9,13]. Thus, the unbinding transition should be observed if driven particles are inserted in these systems, for instance, dielectric colloids manipulated with a laser beam to simulate an external force [25,26]. Motile particles can also simulate an external force; for example, a few colloidal rollers, which are used as a model active matter system [27] could be incorporated in narrow channels with passive colloids. At a larger scale, a mixture of active and passive vibrated disks can be confined to a circular channel [28–30].

The work of O. B. is supported by the European Research Council (Grant No. FPTOpt-277998). We acknowledge discussions with D. Bartolo and S. Ciliberto about the possible experimental tests of our theoretical results.

[1] A. Finkelstein and O. S. Andersen, The gramicidin a channel: A review of its permeability characteristics with special reference to the single-file aspect of transport, J. Membr. Biol. **59**, 155 (1981).
[2] G. Hummer, J. C. Rasaiah, and J. P. Noworyta, Water conduction through the hydrophobic channel of a carbon nanotube, Nature (London) **414**, 188 (2001).
[3] A. Berezhkovskii and G. Hummer, Single-File Transport of Water Molecules through a Carbon Nanotube, Phys. Rev. Lett. **89**, 064503 (2002).
[4] A. Kalra, S. Garde, and G. Hummer, Osmotic water transport through carbon nanotube membranes, Proc. Natl. Acad. Sci. U.S.A. **100**, 10175 (2003).
[5] M. Tokarz, B. Ăkerman, J. Olofsson, J.-F. Joanny, P. Dommersnes, and O. Orwar, Single-file electrophoretic transport and counting of individual DNA molecules in surfactant nanotubes, Proc. Natl. Acad. Sci. U.S.A. **102**, 9127 (2005).
[6] R. H. Tunuguntla, R. Y. Henley, Y.-C. Yao, T. A. Pham, M. Wanunu, and A. Noy, Enhanced water permeability and tunable ion selectivity in subnanometer carbon nanotube porins, Science **357**, 792 (2017).
[7] V. Kukla, J. Kornatowski, D. Demuth, I. Girnus, H. Pfeifer, L. V. C. Rees, S. Schunk, K. K. Unger, and J. Kärger, NMR studies of single-file diffusion in unidimensional channel zeolites, Science **272**, 702 (1996).
[8] D. G. Levitt, Dynamics of a single-file pore: Non-Fickian behavior, Phys. Rev. A **8**, 3050 (1973).
[9] Q. H. Wei, C. Bechinger, and P. Leiderer, Single-file diffusion of colloids in one-dimensional channels, Science **287**, 625 (2000).
[10] T. Meersmann, J. W. Logan, R. Simonutti, S. Caldarelli, A. Comotti, P. Sozzani, L. G. Kaiser, and A. Pines, Exploring single-file diffusion in one-dimensional nanochannels by laser-polarized 129Xe NMR spectroscopy, J. Phys. Chem. A **104**, 11665 (2000).
[11] M. Kollmann, Single-File Diffusion of Atomic and Colloidal Systems: Asymptotic Laws, Phys. Rev. Lett. **90**, 180602 (2003).
[12] C. Lutz, M. Kollmann, and C. Bechinger, Single-File Diffusion of Colloids in One-Dimensional Channels, Phys. Rev. Lett. **93**, 026001 (2004).
[13] B. Lin, M. Meron, B. Cui, S. A. Rice, and H. Diamant, From Random Walk to Single-File Diffusion, Phys. Rev. Lett. **94**, 216001 (2005).
[14] S. F. Burlatsky, G. Oshanin, M. Moreau, and W. P. Reinhardt, Motion of a driven tracer particle in a one-dimensional symmetric lattice gas, Phys. Rev. E **54**, 3165 (1996).
[15] C. Landim, S. Olla, and B. S. Volchan, Driven tracer particle in one dimensional symmetric simple exclusion, Commun. Math. Phys. **192**, 287 (1998).
[16] P. L. Krapivsky, K. Mallick, and T. Sadhu, Large Deviations in Single-File Diffusion, Phys. Rev. Lett. **113**, 078101 (2014).
[17] T. Imamura, K. Mallick, and T. Sasamoto, Large Deviations of a Tracer in the Symmetric Exclusion Process, Phys. Rev. Lett. **118**, 160601 (2017).
[18] J. Cividini, A. Kundu, S. N. Majumdar, and D. Mukamel, Correlation and fluctuation in a random average process on an infinite line with a driven tracer, J. Stat. Mech. (2016) 053212.
[19] A. Kundu and J. Cividini, Exact correlations in a single-file system with a driven tracer, Europhys. Lett. **115**, 54003 (2016).
[20] See Supplemental Material at http://link.aps.org/supplemental/10.1103/PhysRevLett.120.070601 for detailed calculations, which includes Ref. [21].
[21] P. N. Pusey, The dynamics of interacting Brownian particles, J. Phys. A **8**, 1433 (1975).
[22] H. Spohn, *Large Scale Dynamics of Interacting Particles*, Texts and Monographs in Physics (Springer-Verlag, New York, 1991).
[23] T. L. Hill, *An Introduction to Statistical Thermodynamics* (Courier Corporation, North Chelmsford, MA, 1960).
[24] O. Bénichou, A. Bodrova, D. Chakraborty, P. Illien, A. Law, C. Mejía-Monasterio, G. Oshanin, and R. Voituriez, Geometry-Induced Superdiffusion in Driven Crowded Systems, Phys. Rev. Lett. **111**, 260601 (2013).
[25] A. Bérut, A. Petrosyan, and S. Ciliberto, Energy flow between two hydrodynamically coupled particles kept at different effective temperatures, Europhys. Lett. **107**, 60004 (2014).
[26] I. A. Martínez, C. Devailly, A. Petrosyan, and S. Ciliberto, Energy transfer between colloids via critical interactions, Entropy **19**, 77 (2017).
[27] A. Bricard, J.-B. Caussin, N. Desreumaux, O. Dauchot, and D. Bartolo, Emergence of macroscopic directed motion in populations of motile colloids, Nature (London) **503**, 95 (2013).
[28] G. Briand and O. Dauchot, Crystallization of Self-Propelled Hard Discs, Phys. Rev. Lett. **117**, 098004 (2016).
[29] G. Junot, G. Briand, R. Ledesma-Alonso, and O. Dauchot, Active versus Passive Hard Disks against a Membrane: Mechanical Pressure and Instability, Phys. Rev. Lett. **119**, 028002 (2017).
[30] G. Briand, M. Schindler, and O. Dauchot, A flowing crystal of self-propelled particles, arXiv:1709.03844.